

Intramolecular Photoinduced Electron-Transfer Processes in Tetrathienylethylene–Quaterthiophene–[60]Fullerene Triad in Solutions

Ken-ichi Yamanaka,[†] Mamoru Fujitsuka,^{†,§} Yasuyuki Araki,[†] Osamu Ito,^{*,†} Toshihide Aoshima,[‡] Takanori Fukushima,^{‡,||} and Tsutomu Miyashi[‡]

Institute of Multidisciplinary Research for Advanced Materials, Tohoku University, CREST, Japan Science and Technology, Katahira, Sendai, Miyagi 980-8577, Japan, and Department of Chemistry, Graduate School of Science, Tohoku University, Aoba-ku, Sendai, Miyagi 980-8587, Japan

Received: September 30, 2003; In Final Form: November 5, 2003

Intramolecular photoinduced charge-separation and recombination processes in a covalently connected tetrathienylethylene-quaterthiophene- C_{60} (TTE-4T- C_{60}) triad have been studied by time-resolved fluorescence and transient absorption spectral methods. The observed low fluorescence intensity and the short fluorescence lifetime of the C_{60} moiety of the triad in benzonitrile (PhCN) indicate that charge separation takes place via the singlet excited state of the C_{60} moiety in quite fast rate and high efficiency. The nanosecond transient absorption spectra in PhCN showed the broad absorption bands in the 600–1500 nm region, which were attributed to $(TTE-4T)^{+•}-C_{60}^{-•}$, in which the radical cation (hole) delocalizes both on the TTE and 4T moieties. The charge-separated state decays to the neutral triad with a lifetime of 18 ns in PhCN at room temperature. From temperature dependence of the charge-recombination rate constants, the reorganization energy was evaluated to be 0.74 eV, which indicates that the charge-recombination process is in the inverted region of the Marcus parabola. In toluene, $TTE-4T^{-1}C_{60}^{*}$ predominantly descends to $TTE-4T^{-3}C_{60}^{*}$, which decays to the ground state.

Introduction

Since buckminsterfullerene C_{60} has been discovered as a very attractive electron acceptor with unique photophysical and electrochemical properties,^{1,2} considerable efforts have been devoted in recent years to develop the systems in which C_{60} is covalently linked to electron donors,^{3–12} in addition to the mixture systems of C_{60} and donor.^{13–20} Such molecular assemblies are of particular interest, because they can exhibit characteristic electronic properties in the excited-states;^{3–20} thus, a lot of researches have been conducted to the photoinduced electron-transfer processes including C_{60} .^{3–20} In the intramolecular processes involving electron or energy transfer between electroactive entities, C_{60} has been employed as an electron or energy acceptor of special interest, because of its symmetry, large spherical shape, and the properties of its unique π -electron system.^{3–12} These phenomena open the potential applications in the realization of new artificial photosynthetic systems, molecular electronic devices, and photovoltaic cells.^{3,5–7}

Among the wide variety of donor molecules that can be covalently linked to C_{60} , one of the fascinating donors is tetrathiafluvalene (TTF) and its derivatives; various TTF-connected C_{60} dyads have been synthesized and the photoinduced processes were revealed.^{21–24} Recently, tetrathienylethylenes (TTEs) were synthesized as two electron donors.^{25,26} It is reported that TTEs act as good electron donors for C_{60} in the mixture system in benzonitrile (PhCN).²⁷ Other interesting donors are oligothiophenes (nT); various nT -connected C_{60}

dyads have been investigated.^{11,12} In our previous studies, we reported that the 4T- C_{60} dyad showed a quite persistent charge-separated state in PhCN.¹¹ In the present study, a tetrathienylethylene-quaterthiophene- C_{60} triad (TTE-4T- C_{60} in Scheme 1) was synthesized; it is expected that the TTE and 4T moieties act as electron donors to the singlet excited state of C_{60} acting as electron acceptor. The charge-separation and recombination processes were investigated by the time-resolved fluorescence and absorption spectra in the visible and near-IR regions. The temperature effect on the charge-recombination rate-constants gave valuable information for electron-transfer process of the triad.

Experimental Section

Materials. [60]Fullerene (C_{60}) was obtained from MER Corporation, (99.5% purity). PhCN, toluene, *n*-hexane, benzene- d_6 , *N*-methyl glycine, and α -cyano-4-hydroxycinnamic acid were purchased from Aldrich Chemicals (Milwaukee, WI).

Synthesis of TTE-4T- C_{60} . TTE-4T- C_{60} was synthesized from C_{60} (40 mg, 0.056 mmol), TTE-4T-CHO (30 mg, 0.027 mmol; see Supporting Information about the preparation), and *N*-methylglycine (25 mg, 0.28 mmol) in toluene (50 mL) by the Prato method according to eq 1.²⁸ A reaction mixture was refluxed in the dark for 1 day, then the solvent was evaporated under vacuum. The reaction mixture was purified by column chromatography (silica gel, toluene/*n*-hexane = 1:1). Recrystallization from toluene-methanol gave TTE-4T- C_{60} as a brown solid in 30% yield. ¹H NMR (400 MHz, C_6D_6) δ 7.34 (s, 1H), 7.21–6.65 (overlapped peaks, 13H), 4.95 (s, 1H), 4.83 (s, 1H), 3.75 (s, 1H), 2.65 (s, 3H), 2.57 (t, 4H), 1.98 (s, 3H), 1.97 (s, 3H), 1.95 (s, 3H), 1.40 (m, 4H), 1.20 (m, 20H), 0.88 (m, 6H); ¹³C NMR (100 MHz, C_6D_6) δ 6.76, 18.01, 30.95, 43.02, 55.12, 57.01, 63.46, 65.47, 67.07, 79.14, 81.15, 82.76,

* Corresponding author. E-mail: ito@tagen.tohoku.ac.jp.

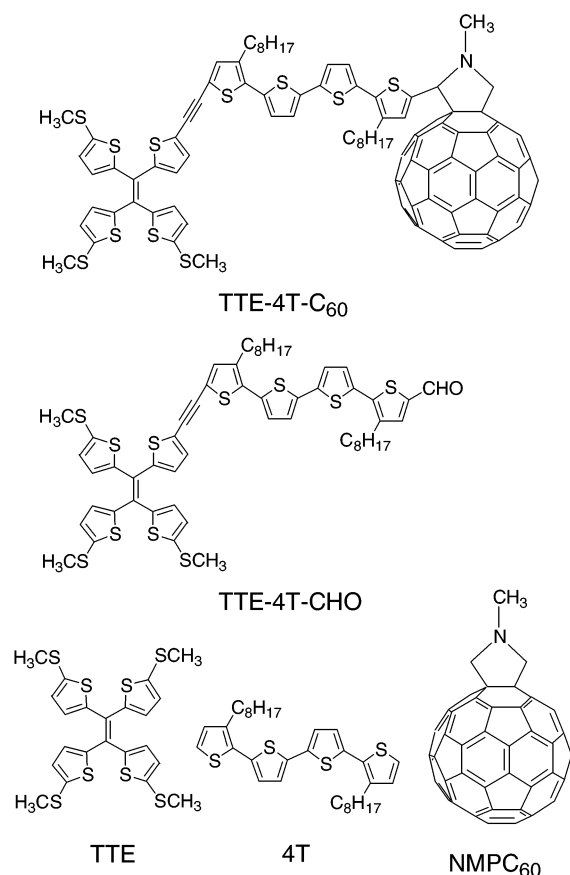
[†] IMRAM, Tohoku University.

[‡] Department of Chemistry, Tohoku University.

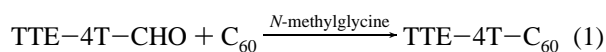
[§] Present address: The Institute of Scientific and Industrial Research, Osaka University, Osaka, Japan.

^{||} Present address: ERATO Nanospace Project, JST, Tokyo, Japan.

SCHEME 1



84.36, 89.65, 91.60, 93.21, 94.82, 103.67, 105.277, 110.51, 112.11, 113.73, 115.56, 118.95, 129.08, 137.86, 139.75, 145.10, 146.70, 147.10, 151.92, 153.53, 164.00, 165.60; MALDI-TOF-MS m/z 1847.86 (M⁺).



Measurements. Electrochemical Measurements. Reduction potentials (E_{red}) and oxidation potentials (E_{ox}) were measured by cyclic voltammetry with a potentiostat (BAS CV50W) in a conventional three-electrode cell equipped with Pt-working and counter electrodes with an Ag/Ag⁺ reference electrode at scan rate of 100 mV/s. The E_{red} and E_{ox} were expressed vs. ferrocene/ferrocenium (Fc/Fc⁺) used as internal reference. In each case, a solution containing 0.2 mM of a sample with 0.05 M of *n*-Bu₄NClO₄ (Fluka purest quality) was deaerated with argon bubbling before measurements.

Steady-State Measurements. Steady-state absorption spectra in the visible and near-IR regions were measured on a Jasco V570 DS spectrophotometer. Steady-state fluorescence spectra were measured on a Shimadzu RF-5300 PC spectrofluorophotometer equipped with a photomultiplier tube having high sensitivity in the 700–800 nm region.

Time-Resolved Fluorescence Measurements. The time-resolved fluorescence spectra were measured by single photon counting method using a streakscope (Hamamatsu Photonics, C4334-01) as a detector and the laser light (second harmonic generation (SHG), 410 nm) of a Ti:sapphire laser (Spectra-Physics, Tsunami 3950-L2S, 1.5 ps fwhm) as an excitation source.^{11,17,29} Lifetimes were evaluated with software provided with the equipment.

Nanosecond Transient Absorption Measurements. Nanosecond transient absorption measurements were carried out using

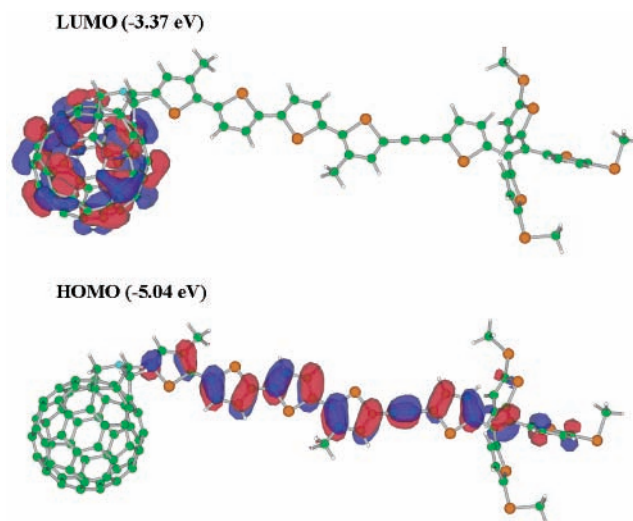


Figure 1. Optimized structures and electron distributions of LUMO and HOMO calculated at the B3LYP/3-21G level.

SHG (532 nm) of a Nd:YAG laser (Spectra-Physics, Quanta-Ray GCR-130, 5 ns fwhm) as an excitation source. For transient absorption spectra in the near-IR region (600–1200 nm) and the time profiles, monitoring light from a pulsed Xe lamp was detected with a Ge-APD (Hamamatsu Photonics, B2834). For spectra in the visible region (400–1000 nm), a Si-PIN photodiode (Hamamatsu Photonics, S1722-02) was used as a detector.^{11,17,27,29}

Molecular Orbital Calculations. The optimized structure, energy levels of the molecular orbitals, and electron densities were calculated using GAUSSIAN 98 at the B3LYP/3-21G level.

Results and Discussion

Molecular Orbital Calculations. In Figure 1, the optimized structure and the electron densities of the lowest unoccupied molecular orbital (LUMO) and the highest occupied molecular orbital (HOMO) of TTE-4T-C₆₀ triad are shown. The optimized structure shows that one thiophene ring of TTE and 4T moieties are coplanar, suggesting possible delocalization of the electrons over these moieties. Indeed, the calculated electron densities of the HOMO indicate the delocalization of electrons in both 4T and TTE moieties, indicating that the 4T and TTE moieties behave as one-donor groups, which also suggests the hole distribution in the charge-separated state. On the other hand, the electron densities in the LUMO are all located on the C₆₀ moiety, suggesting that C₆₀ acts as the acceptor in the triad.

Electrochemical Measurements. The cyclic voltammogram of TTE-4T-C₆₀ in PhCN is shown in Figure 2. An almost reversible pattern was observed, suggesting the stability of the radical ions. The E_{ox} values were evaluated to be 0.21 and 0.52 V vs. Fc/Fc⁺. Compared with the E_{ox} values of the pristine TTE ($E_{\text{ox}} = +0.15$ V vs Fc/Fc⁺) and pristine 4T ($E_{\text{ox}} = +0.59$ V vs Fc/Fc⁺), the E_{ox} values of the TTE-4T moiety in TTE-4T-C₆₀ shifted so that the potential difference became small, suggesting appreciable interaction between 4T and TTE moieties in TTE-4T-C₆₀. In addition, these peaks are broader than those of the corresponding isolated components, which also suggests a considerable interaction between the TTE and 4T moieties.

The reduction potential (E_{red}) of TTE-4T-C₆₀ was evaluated to be -1.08 V vs Fc/Fc⁺; this value corresponds to E_{red} of the C₆₀ moiety, since a quite similar value was reported for NMPC₆₀ ($E_{\text{red}} = -1.10$ V vs Fc/Fc⁺).³⁰ From these observed E_{ox} and E_{red} values for TTE-4T-C₆₀, the free-energy changes for

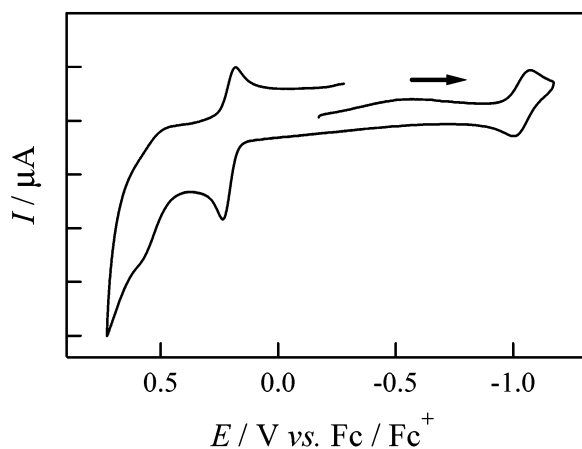


Figure 2. Cyclic voltammogram of TTE-4T-C₆₀ (0.2 mM) in Ar-saturated PhCN containing Bu₄NClO₄ (0.05 M) as a supporting electrolyte at scan rate of 0.1 V s⁻¹.

charge-separation (ΔG_{CS}) and charge-recombination (ΔG_{CR}) can be calculated from the Weller equation:³¹

$$-\Delta G_{CS} = \Delta E_{0-0} - (-\Delta G_{CR}) \quad (2)$$

$$-\Delta G_{CR} = E_{ox} - E_{red} + \Delta G_S \quad (2)$$

$$-\Delta G_S =$$

$$\frac{e^2}{4\pi\epsilon_0} \left[\left(\frac{1}{2R^+} + \frac{1}{2R^-} - \frac{1}{R_{cc}} \right) \left(\frac{1}{\epsilon_s} \right) - \left(\frac{1}{2R^+} + \frac{1}{2R^-} \right) \left(\frac{1}{\epsilon_r} \right) \right] \quad (4)$$

where ΔE_{0-0} is referred to energy of the 0-0 transition, R^+ to radii of the radical cations, R^- to radius of the radical anion, and R_{cc} to center-to-center distance between donor and acceptor (Table 1). The terms e , ϵ_0 , ϵ_s , and ϵ_r refer to elementary charge, vacuum permittivity, and static permittivities of the solvents used for rate measurements and redox potential measurements, respectively. The ΔG_{CS} and ΔG_{CR} values for TTE-4T-C₆₀ in PhCN are summarized in Table 1.

Steady-State Absorption Measurements. Steady-state absorption spectra of TTE-4T-C₆₀ and its components in toluene are shown in Figure 3. The broad absorption bands at 640 and 710 nm of TTE-4T-C₆₀ are characteristic of the 58 conjugated π -electrons of the C₆₀ moiety. These absorption bands in the visible region are essentially the same as those of NMPC₆₀.^{17c} The absorption intensities of TTE-4T-CHO in the region of 300-550 nm are quite larger than the summation of the absorptions of the TTE and 4T, which suggests appreciable interaction between the TTE and 4T moieties in TTE-4T-CHO. For TTE-4T-C₆₀, the absorption intensity around 450-550 nm was almost the same as that of TTE-4T-CHO, indicating that delocalization of the electrons between the TTE and 4T moieties is kept in TTE-4T-C₆₀. From the MO

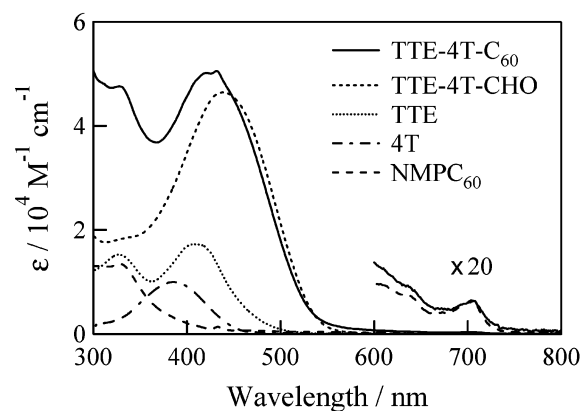


Figure 3. Steady-state absorption spectra of TTE-4T-C₆₀, TTE-4T-CHO, TTE, 4T and NMPC₆₀ in toluene.

calculation, the charge-transfer band would be anticipated in a wavelength region longer than 700 nm; however, the absorption intensity is too low to observe explicitly.

Steady-State Fluorescence Measurement. The steady-state fluorescence spectrum of TTE-4T-C₆₀ in toluene exhibits the fluorescence peak (λ_f) at 720 nm as shown in Figure 4a. Since the spectral shape of the fluorescence band of TTE-4T-C₆₀ is almost the same as that of NMPC₆₀ in the same solvent ($\lambda_f = 717$ nm), the origin of the observed fluorescence of TTE-4T-C₆₀ is the C₆₀ moiety. From the fluorescence peak, the lowest singlet excited energy of the C₆₀ moiety was estimated to be 1.72 eV. The fluorescence intensity of TTE-4T-C₆₀ in toluene is almost the same as that of NMPC₆₀, when the absorbance at excitation wavelength was matched.

In polar solvents such as PhCN, the fluorescence intensity of TTE-4T-C₆₀ becomes lower than those of NMPC₆₀ in the same solvent as shown in Figure 4b. Such a decrease in the fluorescence intensity of TTE-4T-C₆₀ in polar solvent suggests the electron transfer via the singlet excited state of the C₆₀ (¹C₆₀^{*}) moiety.

Fluorescence Lifetimes. In Figure 5, the time profiles of the fluorescence intensity at the peak position of the ¹C₆₀^{*} moiety in TTE-4T-C₆₀ in toluene and PhCN are shown. In toluene, after quick decay, the fluorescence decay of the ¹C₆₀^{*} moiety obeys a single-exponential function, yielding the fluorescence lifetime of 1300 ps, which is the same as that of NMPC₆₀.^{17c} This finding indicates that both energy- and electron-transfers do not take place. In PhCN, the fluorescence of the ¹C₆₀^{*} moiety in TTE-4T-C₆₀ shows biexponential decay, giving a short fluorescence lifetime ($\tau_f < 10$ ps) and long one ($\tau_f = 63$ ps). In both solvents, an initial quick decay of less than 10 ps was observed; since such a quick decay is almost the same as the instrumental limit, further analysis was not performed. Probably, energy transfer and/or electron transfer may be possible from the singlet excited states of the TTE and 4T moieties.

TABLE 1: Center-to-Center Distance (R_{CC}), Free-Energy Change for Charge Separation ($-\Delta G_{CS}$), and Free Energy Change for Charge Recombination ($-\Delta G_{CR}$) of TTE-4T-C₆₀

initial state	final state	solvent	$R_{CC}/\text{\AA}$ ^a	$-\Delta G_{CS}/\text{eV}$ ^b	$-\Delta G_{CR}/\text{eV}$ ^b
TTE-4T- ¹ C ₆₀ [*]	TTE-4T ^{•+} -C ₆₀ ^{•-}	PhCN	13	0.20	1.52
TTE-4T- ¹ C ₆₀ [*]	TTE ^{•+} -4T-C ₆₀ ^{•-}	PhCN	30	0.49	1.23
TTE-4T- ¹ C ₆₀ [*]	(TTE-4T) ^{•+} -C ₆₀ ^{•-}	PhCN	22	0.50	1.22 ^c
TTE-4T- ¹ C ₆₀ [*]	TTE-4T ^{•+} -C ₆₀ ^{•-}	toluene	13	-0.39	2.11
TTE-4T- ¹ C ₆₀ [*]	TTE ^{•+} -4T-C ₆₀ ^{•-}	toluene	30	-0.27	1.99
TTE-4T- ¹ C ₆₀ [*]	(TTE-4T) ^{•+} -C ₆₀ ^{•-}	toluene	22	-0.07	1.79 ^c

^a Evaluated from the optimized structure (Figure 1) calculated by MO method. ^b Calculated from eqs 2-4 employing $\Delta E_{0-0} = 1.72$ eV, $E_{ox} = 0.21$ V for TTE, $E_{ox} = 0.52$ V for 4T, and $E_{red} = 1.08$ V for C₆₀ vs. Fc/Fc⁺. $R^+ = 9.6$ Å for TTE, 7.5 Å for 4T, and 17.3 Å for (TTE-4T); $R^- = 4.2$ Å for C₆₀, as evaluated from Figure 1. Permittivities of PhCN and toluene are 25.2 and 2.38, respectively. ^c E_{ox} for (TTE-4T) = (E_{ox} for TTE + E_{ox} for 4T)/2.

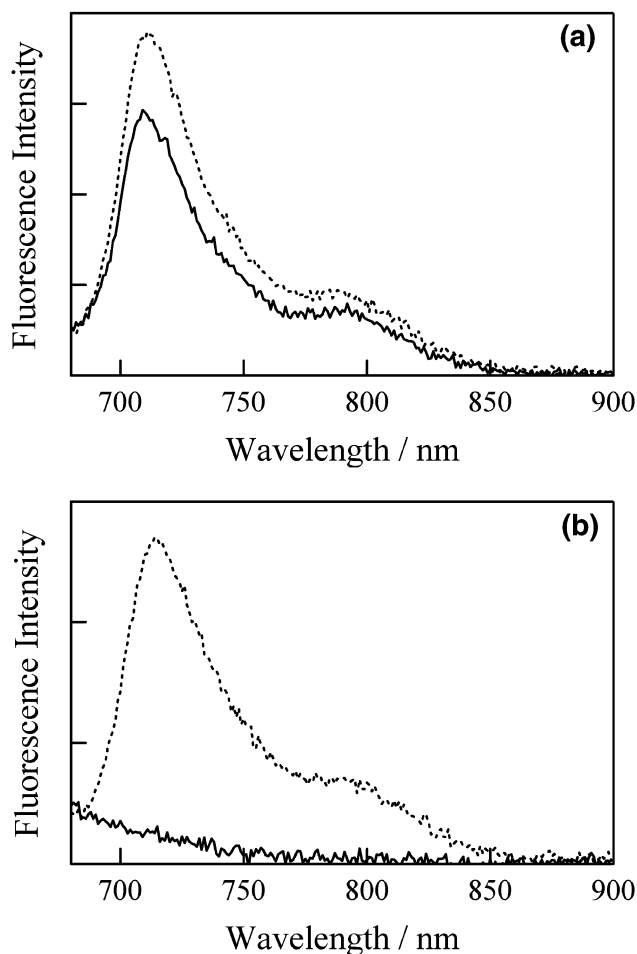


Figure 4. Fluorescence spectra of TTE-4T-C₆₀ (0.1 mM; solid line) and NMPC₆₀ (0.1 mM; dot line) in (a) toluene and (b) PhCN; excitation at 560 nm, where the absorbance of both compounds was matched.

TABLE 2: Fluorescence Lifetime (τ_f at 710–730 nm), Charge-Separation Rate Constant (k_{CS}), Quantum Yield for Charge Separation (Φ_{CS}), Charge-Recombination Rate Constant (k_{CR}) of TTE-4T-C₆₀

compound	solvent	τ_f/s	k_{CS}/s^{-1}	Φ_{CS}	k_{CR}/s^{-1}
TTE-4T-C ₆₀	PhCN	6.3×10^{-11}	1.5×10^{10}	0.95	5.5×10^7

The difference between the τ_f values evaluated from the main decays in 710–730 nm in polar and nonpolar solvents can be attributed predominantly to charge separation via the ¹C₆₀* moiety in TTE-4T-C₆₀, since energy transfer from the ¹C₆₀* moiety to the TTE-4T moiety is impossible from the comparison of the energies of their excited singlet states ($\Delta E_{0-0} = 2.70$ and 2.76 eV for 4T and TTE, respectively).^{11b,27} The intramolecular charge-separation in PhCN may occur from the TTE, 4T, and/or TTE-4T moieties to the ¹C₆₀* moiety in TTE-4T-C₆₀, forming the radical ion-pair states (TTE^{•+}-4T-C₆₀^{•-}, TTE-4T^{•+}-C₆₀^{•-}, and/or (TTE-4T)^{•+}-C₆₀^{•-}, respectively).

From the τ_f value (63 ps) of the ¹C₆₀* moiety in TTE-4T-C₆₀, the intramolecular charge-separation rate constant (k_{CS}) in PhCN was evaluated as summarized in Table 2 using eq 5^{11b,c}

$$k_{CS} = \frac{1}{\tau_f} - \frac{1}{\tau_0} \quad (5)$$

where τ_0 is the fluorescence lifetime of NMPC₆₀ in PhCN.^{17e} Thus, the k_{CS} value was evaluated to be $1.5 \times 10^{10} s^{-1}$ in PhCN,

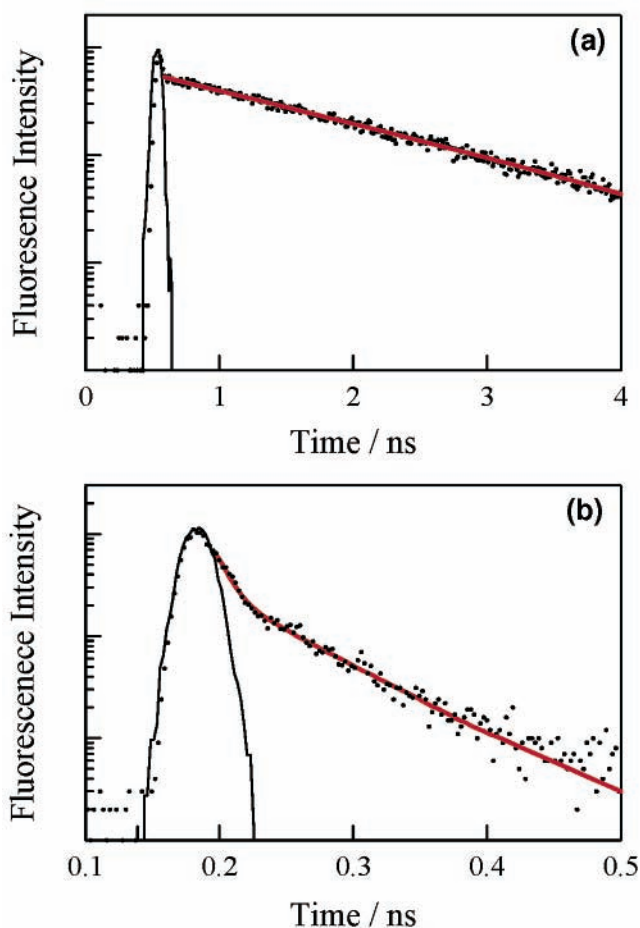


Figure 5. Fluorescence decay profiles around 710–730 nm of TTE-4T-C₆₀ in (a) toluene and (b) PhCN after 410-nm laser irradiation. Solid lines indicate laser profile. Red curves are fitting curves.

which indicates that charge separation process via the ¹C₆₀* moiety is quite fast in polar solvents. The quantum yield of charge separation (Φ_{CS}) via the ¹C₆₀* moiety in TTE-4T-C₆₀ in PhCN was evaluated from eq 6^{11b,c}

$$\Phi_{CS} = \frac{k_{CS}}{k_{CS} + k_0} = \frac{(\tau_f)^{-1} - (\tau_0)^{-1}}{(\tau_f)^{-1}} \quad (6)$$

where k_0 is the fluorescence decay rate of NMPC₆₀. Thus, $\Phi_{CS} = 0.95$ was calculated for TTE-4T-C₆₀ in PhCN, which indicates that charge separation is almost quantitative in PhCN.

Nanosecond Transient Absorption Measurements. Transient absorption spectra observed by the nanosecond laser excitation (532 nm) of TTE-4T-C₆₀ in PhCN are shown in Figure 6. The broad absorption bands were observed in the region of 600–1600 nm, which is the overlapping region of the absorption bands of C₆₀^{•-} (1000 nm),^{17e} TTE^{•+} (1100 nm),²⁷ and 4T^{•+} (680 and 1100 nm) moieties.³² However, these radical ions do not have absorption bands longer than 1100 nm, which suggests appreciable interaction between these radical ions of TTE and 4T, producing the (TTE-4T)^{•+} moiety. After photoexcitation, conformation of the TTE-4T moiety may change to be favorable to the delocalization of hole. From the time profile at 1000 nm, the charge-recombination rate constant (k_{CR}) was evaluated to be $5.5 \times 10^7 s^{-1}$, from which the lifetime of the charge-separated state was calculated to be 18 ns at room temperature.³³ Thus, the ratio of k_{CS}/k_{CR} was evaluated to be

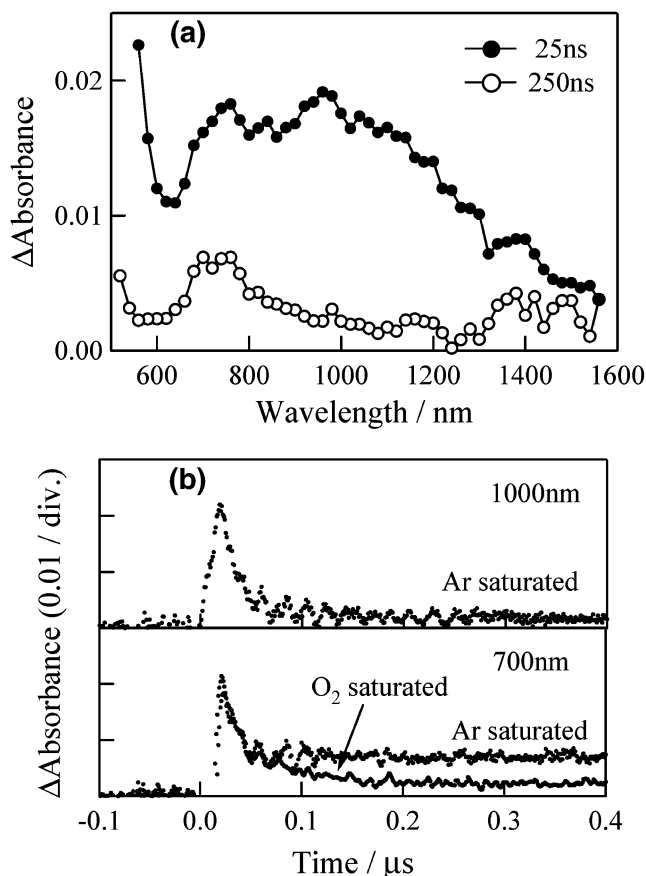


Figure 6. (a) Nanosecond transient absorption spectra of TTE-4T- C_{60} (0.1 mM) in Ar-saturated PhCN at 25 and 250 ns after 532-laser irradiation. (b) Time profiles at 1000 and 700 nm in Ar-saturated and O_2 -saturated PhCN.

270, which is larger than that reported for TTF- C_{60} dyads ($k_{CS}/k_{CR} = 50-150$ in PhCN),^{24b} indicating that TTE-4T- C_{60} is an efficient charge-separation system in polar solvents.

After quick decay of the charge-separated state, the absorption bands remained around 700 nm at 250 ns (Figure 6), which indicates that the absorption band of TTE-4T- ${}^3C_{60}^*$ was hidden in the broad absorption in 600-1600 nm at 25 ns. The decay time profile at 700 nm has two components as shown in inset of Figure 6b; the fast decay part with short lifetime (18 ns) is attributed to the charge-recombination process between the (TTE-4T) $^{+}$ and C_{60}^{*-} moieties, while the slow decay part is ascribed to the decay of the ${}^3C_{60}^*$ moiety, because the slow decay rate was accelerated on addition of O_2 due to energy transfer.^{13,17e} In the transient spectrum at 250 ns, other weak absorption bands in the 900-1500 nm region are difficult to assign.

By the excitation with the 355-nm laser light, transient absorption spectra similar to Figure 6 were observed. Since the 355-nm laser light excites three moieties of the triad in almost equal amounts, as estimated from Figure 3, it is difficult to presume that charge separation takes place via the singlet excited states of the TTE and 4T moieties in addition to ${}^1C_{60}^*$. Since the excitation with the 355-nm light seems to slightly induce photodissociation, further study was not performed.

In toluene, a transient absorption band was observed around 700 nm at 50 ns (Figure 7a). The possible species of the absorption band are the ${}^3C_{60}^*$ moiety (700 nm) and the $4T^{+}$ moiety (680 nm);^{11b} in the present case, the absorption band at 700 nm was ascribed to TTE-4T- ${}^3C_{60}^*$, since the decay rate at 700 nm was accelerated on addition of O_2 (Figure 7b).^{17e}

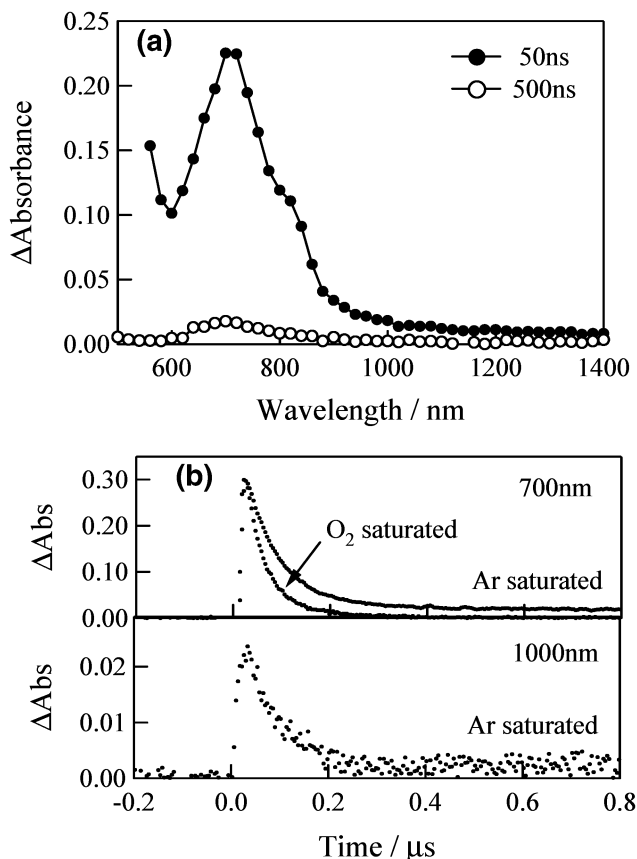


Figure 7. (a) Nanosecond transient absorption spectra of TTE-4T- C_{60} (0.1 mM) in Ar-saturated toluene at 50 and 500 ns after 532-laser irradiation. (b) Time profiles at 700 and 1000 nm in Ar-saturated and O_2 -saturated PhCN.

The weak absorption near 1000 nm was also ascribed to the tail of the huge 700 nm band of the ${}^3C_{60}^*$ -moiety, since the decay time profile was quite similar to that at 700 nm. Thus, the charge-separated state was not observed in the time region longer than the laser light pulse (ca. 5 ns) in the present study. This observation was supported by the positive ΔG_{CS} value in toluene (Table 1), suggesting difficulty of charge separation. It should be noted that the time profile at 700 nm seems to have two components; the lifetime evaluated from the fast component of TTE-4T- ${}^3C_{60}^*$ (0.12 μs) was quite shorter than lifetimes of the triplet states of pristine ${}^3C_{60}^*$ and the ${}^3NMP C_{60}^*$ derivatives (10-30 μs),^{17e} although the lifetime evaluated from minor slow decay part was as long as ca. 10 μs . Although the mechanism for the fast decay process is unclear in the present stage of our study, the following possibilities can be pointed out. (1) The fast decay part may result from the mixing of TTE-4T- ${}^3C_{60}^*$ with the charge-separated states; thus, the very short lifetime of the charge-separated states in toluene may be crippling the lifetime of TTE-4T- ${}^3C_{60}^*$. (2) A bimolecular process such as triplet-triplet annihilation between TTE-4T- ${}^3C_{60}^*$ molecules in toluene may shorten the apparent triplet lifetime.

Temperature Effect. The energy barrier for the charge-recombination process can be estimated by measuring the temperature dependence of k_{CR} . From the semiclassical Marcus equation,³⁴ the electron-transfer rate constant (k) can be described as follows:

$$\ln(k\sqrt{T}) = \ln\left(\frac{2\pi^{3/2}|V|^2}{h\sqrt{\lambda k_B}}\right) - \frac{\Delta G^\ddagger}{k_B T} \quad (7)$$

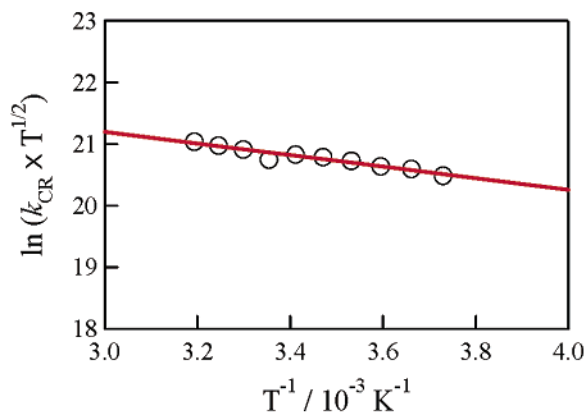


Figure 8. Semiclassical Marcus (modified Arrhenius) plots of the temperature dependence of k_{CR} for TTE-4T-C₆₀ in PhCN.

TABLE 3: Gibbs Activation Energy (ΔG_{CR}^\ddagger), Reorganization Energy (λ), and Electron-Coupling Matrix Element ($|V|$) for Charge-Recombination Process of TTE-4T-C₆₀

compound	solvent	$\Delta G_{CR}^\ddagger/\text{eV}$	λ/eV	$ V /\text{cm}^{-1}$
TTE-4T-C ₆₀	PhCN	0.081	0.74	2.3

where T , $|V|$, h , λ , k_B , and ΔG^\ddagger are referred to as absolute temperature, electron coupling matrix element, Planck constant, reorganization energy, Boltzmann constant, and the Gibbs activation energy in the Marcus theory,³⁴ respectively. The observed k_{CR} values decreased with temperature from $2 \times 10^8 \text{ s}^{-1}$ at 40 °C to $4.5 \times 10^7 \text{ s}^{-1}$ at -15 °C, which were larger changes than the experimental error ($\pm 5\%$). Figure 8 shows the modified Arrhenius plot for the semiclassical Marcus eq 7,³⁴ which shows a linear relation between $\ln(k_{CR}T^{1/2})$ values and $1/T$. From the slope, i.e., $(-\Delta G_{CR}^\ddagger / k_B)$, the ΔG_{CR}^\ddagger value was estimated to be 0.081 eV (Table 3). The λ value for the charge-recombination process was calculated to be 0.74 eV from the following relation:³⁴

$$\Delta G^\ddagger = \frac{(\Delta G_{CR} + \lambda)^2}{4\lambda} \quad (8)$$

From the comparison of the λ ($= 0.74 \text{ eV}$) with ΔG_{CR} value (-1.22 to -1.52 eV in PhCN in Table 1), the charge-recombination processes are considered to be in the Marcus “inverted region”.³⁴ These findings indicate that the rate constant of charge recombination is relatively slower than those of other dyads.⁵⁵ The $|V|$ value was calculated to be 2.3 cm^{-1} from the intercept of the slope in Figure 8. This $|V|$ value is similar to the value of the dyad (3.9 cm^{-1} for ZnP-C₆₀)^{6c} rather than that of the triads (0.019 cm^{-1} for ZnP-H₂P-C₆₀)^{6c}, supporting the assumption that the charge-separated state is predominantly (TTE-4T)^{•+}-C₆₀^{•-}.

Energy Diagram. Figure 9 shows an energy diagram of TTE-4T-C₆₀ in PhCN when the 532-nm laser light is used as the excitation light. Energy levels of the radical ion pairs were cited from Table 1. The charge separation takes place via TTE-4T-¹C₆₀^{*} as indicated by the weak fluorescence intensity and short fluorescence lifetime, since the energy levels of TTE-4T^{•+}-C₆₀^{•-}, TTE^{•+}-4T-C₆₀^{•-}, and (TTE-4T)^{•+}-C₆₀^{•-} were lower than TTE-4T-¹C₆₀^{*}. In (TTE-4T)^{•+}-C₆₀^{•-}, hole delocalization may occur between TTE-4T^{•+}-C₆₀^{•-} and TTE^{•+}-4T-C₆₀^{•-} as indicated by the broad transient absorption bands in the nanosecond transient spectra in Figure 6. Since $\Delta G_{CR}^\ddagger = 0.081 \text{ eV}$ is smaller than the energy difference between

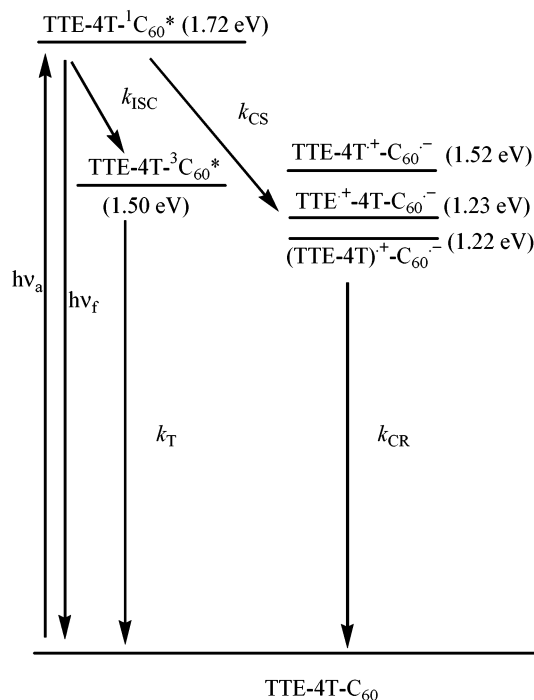


Figure 9. Schematic energy diagram for electron-transfer processes of TTE-4T-C₆₀ in PhCN.

TTE^{•+}-4T-C₆₀^{•-} and TTE-4T^{•+}-C₆₀^{•-} (0.30 eV), the stepwise charge-recombination from TTE^{•+}-4T-C₆₀^{•-} via TTE-4T^{•+}-C₆₀^{•-} may not be possible. Thus, charge recombination via (TTE-4T)^{•+}-C₆₀^{•-} is most probable. As for the generation of TTE-4T-³C₆₀^{*}, intersystem crossing from TTE-4T-¹C₆₀^{*} is most probable; however, it is also possible to generate TTE-4T-³C₆₀^{*} via charge recombination of TTE-4T^{•+}-C₆₀^{•-}, because of downhill process.^{15b} With the excitation of the TTE-4T moiety of TTE-4T-C₆₀ in PhCN, the charge-separation processes may take place too; however, in the present study, information about the processes was not obtained. In toluene, charge separation from ¹C₆₀^{*} did not occur, since the energy levels of TTE-4T^{•+}-C₆₀^{•-}, TTE^{•+}-4T-C₆₀^{•-}, and (TTE-4T)^{•+}-C₆₀^{•-} are higher than that of TTE-4T-¹C₆₀^{*}.

Comparison with Other Systems. The lifetime of the charge-separated state of 4T-C₆₀ (4T^{•+}-C₆₀^{•-}) was evaluated to be 620 ns in PhCN,^{11b} which is quite longer than that of the charge-separate states of TTE-4T-C₆₀. In the case of 4T^{•+}-C₆₀^{•-}, energy level of 4T^{•+}-C₆₀^{•-} is similar to that of 4T-³C₆₀^{*}; thus, 4T^{•+}-C₆₀^{•-} gains the triplet radical ion-pair character by mixing with 4T-³C₆₀^{*}, leading to the long lifetime for charge separation.^{11b} In the case of TTE-4T-C₆₀, the energy levels of TTE^{•+}-4T-C₆₀^{•-}, and (TTE-4T)^{•+}-C₆₀^{•-} are far lower than that of TTE-4T-³C₆₀^{*}; thus, TTE^{•+}-4T-C₆₀^{•-} and (TTE-4T)^{•+}-C₆₀^{•-} may keep the singlet character. Contribution of TTE-4T^{•+}-C₆₀^{•-} to the charge-separation states may be small, because of its higher energy level. Thus, the lifetime of 18 ns for the charge-separate states of TTE-4T-C₆₀ is shorter than that of 4T^{•+}-C₆₀^{•-} with triplet character. However, since the usual donor-acceptor dyads with short distances have lifetimes for the charge-separated states shorter than 1 ns,³⁵ the observed 18 ns for lifetime of the charge-separated state of TTE-4T-C₆₀ is quite long; this can be explained by far negative ΔG_{CR} than λ , which means that the charge-recombination process is far deep in the inverted region of the Marcus parabola.³⁴

Summary

For TTE-4T-C₆₀, the photoinduced charge separation via the excited singlet state was observed in highly polar solvent. The lifetime of 18 ns was evaluated for the radical ion pair(s) of TTE-4T-C₆₀ in PhCN at room temperature. Broad transient absorption bands suggest hole delocalization between the TTE and 4T moieties. The stable charge-separated states such as TTE^{•+}-4T-C₆₀^{•-} and (TTE-4T)^{•+}-C₆₀^{•-} lose a chance to mix with TTE-4T-³C₆₀^{*} with energy higher than TTE^{•+}-4T-C₆₀^{•-} and (TTE-4T)^{•+}-C₆₀^{•-}, which makes the lifetime of the charge-separated states relatively short. However, high ratio of $k_{CS}/k_{CR} = 270$ indicates that TTE-4T-C₆₀ is an efficient photoinduced charge-separation system in polar solvents such as PhCN.

Acknowledgment. This present work was supported by a Grant-in-Aid on Scientific Research from the Ministry of Education, Culture, Sports, Science and Technology of Japan (12875163 and 14050014) and by the Mitsubishi Foundation.

Supporting Information Available: Synthesis of the triad. This material is available free of charge via the Internet at <http://pubs.acs.org>.

References and Notes

- (1) Kroto, H. W.; O'Brien, S. C.; Curl, R. F.; Smalley, R. E. *Nature* **1985**, *318*, 162.
- (2) Krätschmer, W.; Lamb, L. D.; Fostiropoulos, K.; Huffman, D. R. *Nature* **1990**, *347*, 354.
- (3) Liddell, P. A.; Sumida, J. P.; Macpherson, A. N.; Noss, L.; Seely, G. R.; Clark, K. N.; Moore, A. L.; Moore, T. A.; Gust, D. *Photochem. Photobiol.* **1994**, *60*, 537. (b) Imahori, H.; Cardoso, S.; Tatman, D.; Lin, S.; Noss, L.; Seely, G. R.; Sereno, L.; Silber, C.; Moore, T. A.; Moore, A. L.; Gust, D. *Photochem. Photobiol.* **1995**, *62*, 1009. (c) Kuciauskas, D.; Lin, S.; Seely, G. R.; Moore, A. L.; Moore, T. A.; Gust, D.; Drovetskaya, T.; Reed, C. A.; Boyd, P. D. W. *J. Phys. Chem.* **1996**, *100*, 15926.
- (4) Williams, R. M.; Zwier, M. N.; Verhoeven, J. W. *J. Am. Chem. Soc.* **1995**, *117*, 4093.
- (5) Sariciftci, N. S.; Wudl, F.; Heeger, A. J.; Maggini, M.; Scorrano, G.; Prato, M.; Bourassa, J.; Ford, P. C. *Chem. Phys. Lett.* **1995**, *247*, 510.
- (6) (a) Imahori, H.; Hagiwara, K.; Aoki, M.; Akiyama, T.; Taniguchi, S.; Okada, T.; Shirakawa, M.; Sakata, Y. *J. Am. Chem. Soc.* **1996**, *118*, 11771. (b) Imahori, H.; Ozawa, S.; Uchida, K.; Takahashi, M.; Azuma, T.; Ajavakom, A.; Akiyama, T.; Hasegawa, M.; Taniguchi, S.; Okada, T.; Sakata, Y. *Bull. Chem. Soc. Jpn.* **1999**, *72*, 485. (c) Imahori, H.; Tamaki, K.; Guldi, D. M.; Luo, C.; Fujitsuka, M.; Ito, O.; Sakata, Y.; Fukuzumi, S. *J. Am. Chem. Soc.* **2001**, *123*, 2607.
- (7) (a) Samanta, A.; Kamat, P. V. *Chem. Phys. Lett.* **1992**, *199*, 635. (b) Guldi, D. M.; Maggini, M.; Scorrano, G.; Prato, M. *J. Am. Chem. Soc.* **1997**, *119*, 974. (c) Guldi, D. M.; Maggini, M.; Scorrano, G.; Prato, M. *Res. Chem. Intermed.* **1997**, *23*, 561. (d) Thomas, K. G.; Biju, V.; George, M. V.; Guldi, D. M.; Kamat, P. V. *J. Phys. Chem. A* **1998**, *102*, 5341. (e) Guldi, D. M.; Garscia, G. T.; Mattay, J. J. *J. Phys. Chem. A* **1998**, *102*, 9679. (f) Maggini, M.; Guldi, D. M.; Mondini, S.; Scorrano, G.; Paolucci, F.; Ceroni, P.; Roffia, S. *Chem. Eur. J.* **1998**, *4*, 1992. (g) Polese, A.; Mondini, S.; Bianco, A.; Toniolo, C.; Scorrano, G.; Guldi, D. M.; Maggini, M. *J. Am. Chem. Soc.* **1999**, *121*, 3446.
- (8) Lllacay, J.; Veciana, J.; Vidal-Gancedo, J.; Bourdelnde, J. L.; Gonzalez-Moreno, R.; Rovia, C. *J. Org. Chem.* **1998**, *63*, 5201.
- (9) Tkachenko, N. V.; Rantala, L.; Tauber, A. Y.; Helaja, J.; Hynninen, P. V.; Lemmetyinen, H. *J. Am. Chem. Soc.* **1999**, *121*, 9378.
- (10) Schuster, D. I.; Cheng, P.; Wilson, S. R.; Prokhorenko, V.; Katterle, M.; Holzwarth, A. R.; Braslavsky, S. E.; Klihm, G.; Williams, R. M.; Luo, C. *J. Am. Chem. Soc.* **1999**, *121*, 11599.
- (11) (a) Yamashiro, T.; Aso, Y.; Otsubo, T.; Tang, H.; Harima, T.; Yamashita, K. *Chem. Lett.* **1999**, 443. (b) Fujitsuka, M.; Ito, O.; Yamashiro, T.; Aso, Y.; Otsubo, T. *J. Phys. Chem. A* **2000**, *104*, 4876. (c) Fujitsuka, M.; Matsumoto, K.; Ito, O.; Yamashiro, T.; Aso, Y.; Otsubo, T. *Res. Chem. Intermed.* **2001**, *27*, 73. (d) Fujitsuka, M.; Masuhara, A.; Kasai, H.; Oikawa, H.; Nakanishi, H.; Ito, O.; Yamashiro, T.; Aso, Y.; Otsubo, T. *J. Phys. Chem. B*, **2001**, *105*, 9930.
- (12) van Hal, P. A.; Knol, J.; Langeveld-Voss, B. M. W.; Meskers, S. C. J.; Hummelen, J. C.; Janssen, R. A. J. *J. Phys. Chem. A* **2000**, *104*, 5974. (b) Apperloo, J. J.; Langeveld-Voss, B. M. W.; Knol, J.; Hummelen, J. C.; Janssen, R. A. J. *Adv. Mater.* **2000**, *12*, 908. (c) van Hal, P. A.; Beckers, E. H. A.; Meskers, S. C. J.; Janssen, R. A. J.; Jousseme, B.; Blanchard, P.; Roncali, J. *Chem. Eur. J.* **2002**, *8*, 5415. (d) Beckers, E. H. A.; van Hal, P. A.; Dhanabalan, A.; Meskers, S. C. J.; Knol, J.; Hummelen, J. C.; Janssen, R. A. J. *J. Phys. Chem. A* **2003**, *107*, 6218.
- (13) (a) Arbogast, J. W.; Foote, C. S.; Kao, M. *J. Am. Chem. Soc.*, **1192**, *114*, 2277. (b) Foote, C. S. *Top. Curr. Chem.* **1994**, *169*, 347.
- (14) Wang, Y. *J. Phys. Chem.* **1992**, *96*, 764.
- (15) (a) Seshadri, R.; Rao, C. N. R.; Pal, H.; Mukherjee, T.; Mittal, J. P. *Chem. Phys. Lett.* **1993**, *205*, 395. (b) Ghosh, H. N.; Pal, H.; Saper, A. V.; Mittal, J. P. *J. Am. Chem. Soc.* **1993**, *115*, 11722.
- (16) Schaffner, E.; Fischer, H. *J. Phys. Chem.* **1993**, *97*, 13149.
- (17) (a) Watanabe, A.; Ito, O. *J. Phys. Chem.*, **1994**, *98*, 7736. (b) Ito, O.; Sasaki, Y.; Yoshikawa, Y.; Watanabe, A. *J. Phys. Chem.* **1995**, *99*, 9838. (c) Sasaki, Y.; Yoshikawa, Y.; Watanabe, A.; Ito, O. *J. Chem. Soc., Faraday Trans.* **1995**, *91*, 2287. (d) Alam, M. M.; Watanabe, A.; Ito, O. *J. Photochem. Photobiol. A* **1997**, *104*, 59. (e) Luo, C.; Fujitsuka, M.; Watanabe, A.; Ito, O.; Gan, L.; Huang, Y.; Huang, C. H. *J. Chem. Soc., Faraday Trans.* **1998**, *94*, 527.
- (18) (a) Bennati, M.; Grupp, A.; Bäuerle, P.; Mehring, M. *Chem. Phys.* **1994**, *185*, 221. (b) Bennati, M.; Grupp, A.; Bäuerle, P.; Mehring, M. *Mol. Cryst. Liq. Cryst.* **1994**, *256*, 751.
- (19) (a) Ma, B.; Laeson, G. E.; Bunker, C. E.; Kitaygorodskiy, A.; Sun, Y.-P. *Chem. Phys. Lett.* **1995**, *247*, 51. (b) Sun, Y.-P.; Ma, B.; Lawson, G. E. *Chem. Phys. Lett.* **1995**, *233*, 57. (c) Lawson, G. E.; Kitaygorodskiy, A.; Ma, B.; Bunker, C. E.; Sun, Y.-P. *J. Chem. Soc., Chem. Commun.* **1995**, 2225.
- (20) Fukuzumi, S.; Suenobu, T.; Patz, M.; Hirasaka, T.; Itoh, S.; Fujitsuka, M.; Ito, O. *J. Am. Chem. Soc.* **1998**, *120*, 8060.
- (21) (a) Martín, N.; Sánchez, L.; Seoane, C.; Andreu, R.; Garín, J.; Orduna, J. *Tetrahedron Lett.* **1996**, *37*, 5979. (b) Martín, N.; Sánchez, L.; Guldi, D. M. *Chem. Commun.* **2000**, 113. (c) Martín, N.; Pérez, I.; Sánchez, L.; Seoane, C. *J. Org. Chem.* **1997**, *62*, 5690. (d) Herranz, M. A.; Martín, N. *Org. Lett.* **1999**, *1*, 2005. (e) Martín, N.; Sanchez, L.; Herranz, M. A.; Guldi, D. M. *J. Phys. Chem. A* **2000**, *104*, 4648. (f) Herranz, M. A.; Martín, N.; Sánchez, L.; Seoane, C.; Guldi, D. M. *J. Organomet. Chem.* **2000**, *599*, 2. (g) Guldi, D. M.; González, S.; Martín, N.; Antón, A.; Garín, J. Orduna, J. *J. Org. Chem.* **2000**, *65*, 1978. (h) Herranz, M. A.; Illescas, B.; Martín, N.; Luo, C.; Guldi, D. M. *J. Org. Chem.* **2000**, *65*, 5728. (i) González, S.; Martín, N.; Swartz, A.; Guldi, D. M. *Org. Lett.* **2003**, *5*, 557.
- (22) (a) Bouille, C.; Rabreau, J. M.; Hudhomme, P.; Cariou, M.; Jubault, M.; Gorgues, A.; Orduna, J.; Garín, J. *Tetrahedron Lett.* **1997**, *38*, 3909. (b) Hudhomme, P.; Bouille, C.; Rabreau, J. M.; Cariou, M.; Jubault, M.; Gorgues, A. *Synth. Met.* **1998**, *94*, 73.
- (23) Lllacay, J.; Veciana, J.; Vidal-Gancedo, J.; Bourdelande, J. L.; Gonzalez-Moreno, R.; Rovira, C. *J. Org. Chem.* **1998**, *63*, 5201.
- (24) (a) Allard, E.; Delaunay, J.; Cheng, F.; Cousseau, J.; Orduna, J.; Garín, J.; *Org. Lett.* **2001**, *3*, 3503. (b) Allard, E.; Cousseau, J.; Orduna, J.; Garín, J.; Luo, H.; Araki, Y.; Ito, O.; *Phys. Chem. Chem. Phys.* **2002**, *4*, 5944.
- (25) Yamashita, Y.; Yaegashi, H.; Mukai, T. *Tetrahedron Lett.* **1985**, 3579.
- (26) Suzuki, T.; Shiohara, H.; Monobe, M.; Sakimura, T.; Tanaka, S.; Yamashita, Y.; Miyashi, T. *Angew. Chem., Int. Ed. Engl.* **1992**, *31*, 455.
- (27) Yamanaka, K.; Fujitsuka, M.; Ito, O.; Aoshima, T.; Fukushima, T.; Miyashi, T. *Bull. Chem. Soc. Jpn.* **2003**, *76*, 1341.
- (28) Muggini, M.; Scorrano, G.; Prato, M. *J. Am. Chem. Soc.* **1993**, *115*, 9798.
- (29) Yamazaki, M.; Araki, Y.; Fujitsuka, M.; Ito, O. *J. Phys. Chem. A* **2001**, *105*, 8615.
- (30) D'Souza, F.; Deviprasad, G. R.; Zandler, M. E.; Hoang, V. T.; Klykov, A.; El-Khouly, M. E.; Fujitsuka, M.; Ito, O. *J. Phys. Chem. B* **2002**, *106*, 4952.
- (31) Weller, A. *Z. Phys. Chem. Neue Folge* **1982**, *133*, 93.
- (32) Matsumoto, K.; Fujitsuka, M.; Sato, T.; Onodera, S.; Ito, O. *J. Phys. Chem. B* **2000**, *104*, 11632.
- (33) Although the femtosecond laser excitation (388 nm, fwhm 150 fs) of TTE-4T-C₆₀ gave very complex transient spectra in PhCN because of the contribution of the singlet excited state of TTE, the charge-recombination process showed two-step decays as observed for 4T-C₆₀^{11b} and retinyl-C₆₀²⁹.
- (34) (a) Marcus, R. A. *J. Chem. Phys.* **1956**, *24*, 966. (b) Marcus, R. A. *J. Chem. Phys.* **1965**, *43*, 679. (c) Marcus, R. A.; Sutin, N. *Biochim. Biophys. Acta* **1985**, *811*, 265.
- (35) (a) Wasielewski, M. R.; Niemczyk, M. P.; Svec, W. A.; Pewitt, E. B. *J. Am. Chem. Soc.* **1985**, *107*, 1080. (b) Asahi, T.; Ohkohchi, M.; Matsusaka, R.; Mataga, N.; Zhang, R. P.; Osuka, A.; Maruyama, K. *J. Am. Chem. Soc.* **1993**, *115*, 5665. (c) Macpherson, A. N.; Liddele, P. A.; Lin, S.; Noss, L.; Seely, G. R.; DeGraziano, J. M.; Moore, A. L.; Moore, T. A.; Gust, D. *J. Am. Chem. Soc.* **1995**, *117*, 7202.